

# Modulation of Orbital-Angular-Momentum Symmetry of Nondiffractive Acoustic Vortex Beams and Realization Using a Metasurface

Xue Jiang<sup>✉</sup>, Dean Ta,<sup>†</sup> and Weiqi Wang

*Department of Electronic Engineering, Fudan University, Shanghai 200433, China*



(Received 14 June 2020; revised 20 July 2020; accepted 11 August 2020; published 8 September 2020)

Orbital angular momentum (OAM) carried by acoustic vortex attracts extensive research interests due to the possible application such as acoustic tweezer and communications. The OAM in the conventional symmetric acoustic vortex is generally determined by topological charge  $l$ . Here, we provide the beam symmetry as an alternative factor to manipulate the OAM beyond the topological charge. We propose a nondiffractive asymmetric acoustic vortex beam, which can be generated by an acoustic metasurface and modulate the OAM to arbitrary values. Rather than the radially symmetric distribution, the intensity of the asymmetric acoustic vortex is characterized with a crescent shape controlled by the asymmetry parameter  $\alpha$ . The ratio between axial OAM and sound energy on the transverse plane depends on the asymmetry parameter and thus is *not* quantized by the ratio of topological charge  $l$  to wave angular frequency  $\omega$  as in conventional vortex beam. Moreover, we present the realization of the proposed vortex beam by designed metasurface, and reveal the nondiffractive nature of the asymmetric acoustic vortex beam. Our work expands the family of acoustic vortex and demonstrates an alternative route to control acoustic OAM.

DOI: 10.1103/PhysRevApplied.14.034014

## I. INTRODUCTION

Vortex beams are helical waves with the screw-phase dislocation and an amplitude null at the core [1,2], which have been widely investigated in both acoustic [3–8] and optical fields [9–13]. The vortex beams have an azimuthal phase dependence  $\exp(il\varphi)$  with topological charge  $l$  and carry orbital angular momentum (OAM). In acoustic vortex, the carried OAM leads to intriguing properties, which shed light on promising applications such as particle manipulation [7,8,14–18] and acoustic communications [19–21]. Conventionally, acoustic vortex is radially symmetric with bright rings of high intensity. The OAM carried by this symmetric vortex is known to be characterized with topological charge  $l$ , and transferring the OAM from acoustic beam to the illuminated object results in a radiation torque, where the ratio of the OAM transfer to the energy absorption is given by the ratio of topological charge  $l$  to the angular frequency  $\omega$  [4,5,22]. Therefore, the OAM for acoustic waves with the given frequency and energy density can *only* be controlled by changing the topological charge.

In this work, we explore the beam symmetry as an alternative factor to modulate acoustic OAM beyond the topological charge. The asymmetry-based modulation stems from the extrinsic OAM, which generally relates to the

lateral displacement of the vortex [23], yet no shift from the center of each symmetric Bessel mode is required in our design. Whereas the asymmetry of acoustic vortex beams can arise from the inhomogeneity of media [24], the asymmetry of the vortex beam in a homogeneous media has to be produced using a proper source. The asymmetry can extend application of vortex; for example, manipulation of nanodroplets via a nonuniform focused acoustic vortex [25].

Here we introduce the asymmetry to acoustic vortex beam in a homogeneous media by the superposition of symmetric Bessel modes on the source plane. We realize the modulation based on the theoretical design of nondiffractive asymmetric acoustic vortex beam, and present the generation with acoustic metasurface. We reveal that, besides topological charge  $l$ , the OAM also depends on the asymmetry of the vortex beam, which acts as an alternative factor to manipulate the acoustic OAM. We gain insight into the rich singularity behavior of the asymmetric acoustic vortex. Besides the ordinary singularity corresponding to the topological charge  $l$  in the beam center, the asymmetric vortex beam acquires additional singularities on the  $x$  axis, which always come with pairs and show opposite winding numbers. Thus, the effective topological charge of the asymmetric vortex, resulting from the average of multiple vortices, can be noninteger. However, all the topological charges in each superimposed Bessel modes are still integer, which is different from the fractional topological charge studied in previous works [26,27].

\*xuejiang@fudan.edu.cn

<sup>†</sup>tda@fudan.edu.cn

## II. GENERAL FORMULA OF ASYMMETRIC ACOUSTIC VORTEX

We start by considering the Helmholtz equation for the complex velocity potential  $\Psi$  in cylindrical coordinate system,  $(\nabla^2 + k^2)\Psi = 0$ , where  $k = 2\pi/\lambda$  is the wave number of acoustic wave with wavelength  $\lambda$  and angular frequency  $\omega$ . The Helmholtz equation has a solution in the form of Bessel mode [28]:

$$\Psi_l(r, \varphi, z) = \exp(i\kappa z + il\varphi)J_l(\mu r), \quad (1)$$

with  $\kappa$  and  $\mu$  being the axial and radial wave number ( $\kappa^2 + \mu^2 = k^2$ ), and  $J_l$  being the  $l$ th-order Bessel function of the first kind. According to the superposition principle, any linear combination of  $\Psi_l$  is also the solution of the Helmholtz equation. We propose the asymmetric acoustic vortex beam based on linear superposition of the Bessel modes in Eq. (1), with the velocity potential in the initial

plane ( $z = 0$ ) expressed as follows:

$$\psi_l(r, \varphi, z = 0; \alpha) = \sum_m \frac{\alpha^m \exp(il\varphi + im\varphi)}{m!} J_{l+m}(\mu r). \quad (2)$$

Here, the constant  $\alpha$  is a continuous value and assumed to be real and positive, which is shown to govern the asymmetry degree of the vortex. We can reduce Eq. (2) based on the integral [29]:

$$\sum_{k=0}^{\infty} \frac{t^k}{k!} J_{k+\nu}(x) = x^{\nu/2} (x - 2t)^{-\nu/2} J_{\nu}(\sqrt{x^2 - 2tx}). \quad (3)$$

Consider the beam propagation in free space, the resulting acoustic beam at any distance  $z$  follows:

$$\Psi_l(r, \varphi, z; \alpha) = \left[ \frac{\mu r}{\mu r - 2\alpha \exp(i\varphi)} \right]^{l/2} J_l \left\{ \sqrt{\mu r [\mu r - 2\alpha \exp(i\varphi)]} \right\} \exp(il\varphi) \exp(i\kappa z). \quad (4)$$

Equation (4) is the analytic expression of the asymmetric acoustic vortex beam studied in our work. It is observed in Eq. (4) that the asymmetric vortex beam is characterized with the same spiral phase  $\exp(il\varphi)$  and the  $l$ th-order Bessel function as in ordinary symmetric vortex. However, the amplitude distribution and argument in the Bessel function are modified by the dimensionless quantity  $\alpha$ , which is referred to as the asymmetry parameter. In addition to  $\exp(il\varphi)$ , the azimuthal distribution is also controlled by  $\alpha$ , resulting in a nonlinear dependence of the phase on azimuthal angle. The modulation of the argument in the Bessel function gives rise to the asymmetry and unusual singularity behavior discussed in the following.

Figures 1(a) and 1(b) are the intensity and phase distributions of the proposed asymmetric vortex on the initial plane ( $z = 0$ ) with  $l = 1$  and different asymmetry parameter  $\alpha$ . Throughout the paper, the intensity is normalized with the respective maximum value. Compared to the radially symmetric vortex ( $\alpha = 0$ ), the intensity of the asymmetric vortex features the crescent shape, with the bright spot shifted along  $x$  direction while elongated along  $y$  direction. As predicted in our theory, the asymmetry of the vortex increases with  $\alpha$ . Intensity profiles along the  $x$  axis in Fig. 1(a) are plotted on the bottom. In the phase patterns [Fig. 1(b)], there is an expected singularity with topological charge  $l$  located at the beam's center, denoted by the black circles in the insets (enlarged view), with the position  $x_{\text{sin}}^0 = 0$ . In addition, several anomalous pairs of

isolated intensity zeros are readily seen, generating acoustic vortices pairs on the  $x$  axis (denoted by white circles), all of which bear the unit topological charge with opposite chirality on different sides of the origin [30]. These extra singularities induce additional angular momentum in the asymmetric acoustic vortex beam, which renders the asymmetry as a new tuning knob for the modulation of OAM beyond the topological charge.

## III. SINGULARITY BEHAVIOR

The intriguing singularity behavior of the proposed beam can be explained from the theoretical analysis. The asymmetric vortex beam described in Eq. (4) has a finite number of isolated intensity nulls when the Bessel function is zero, namely,

$$\mu r [\mu r - 2\alpha \exp(i\varphi)] = \gamma_l^p \quad (p = 0, \pm 1, \dots), \quad (5)$$

where  $\gamma_l^p$  is the  $p$ th root of the  $l$ th-order Bessel function:  $J_l(\gamma_l^p) = 0$ . The isolated intensity nulls generate acoustic vortices, corresponding to the singularities of the beam. We can obtain the real solution of Eq. (5) when the azimuthal angle is equal to  $\varphi = m\pi$  ( $m = 0, 1, \dots$ ), which indicates that the singularities only locate on the  $x$  axis.

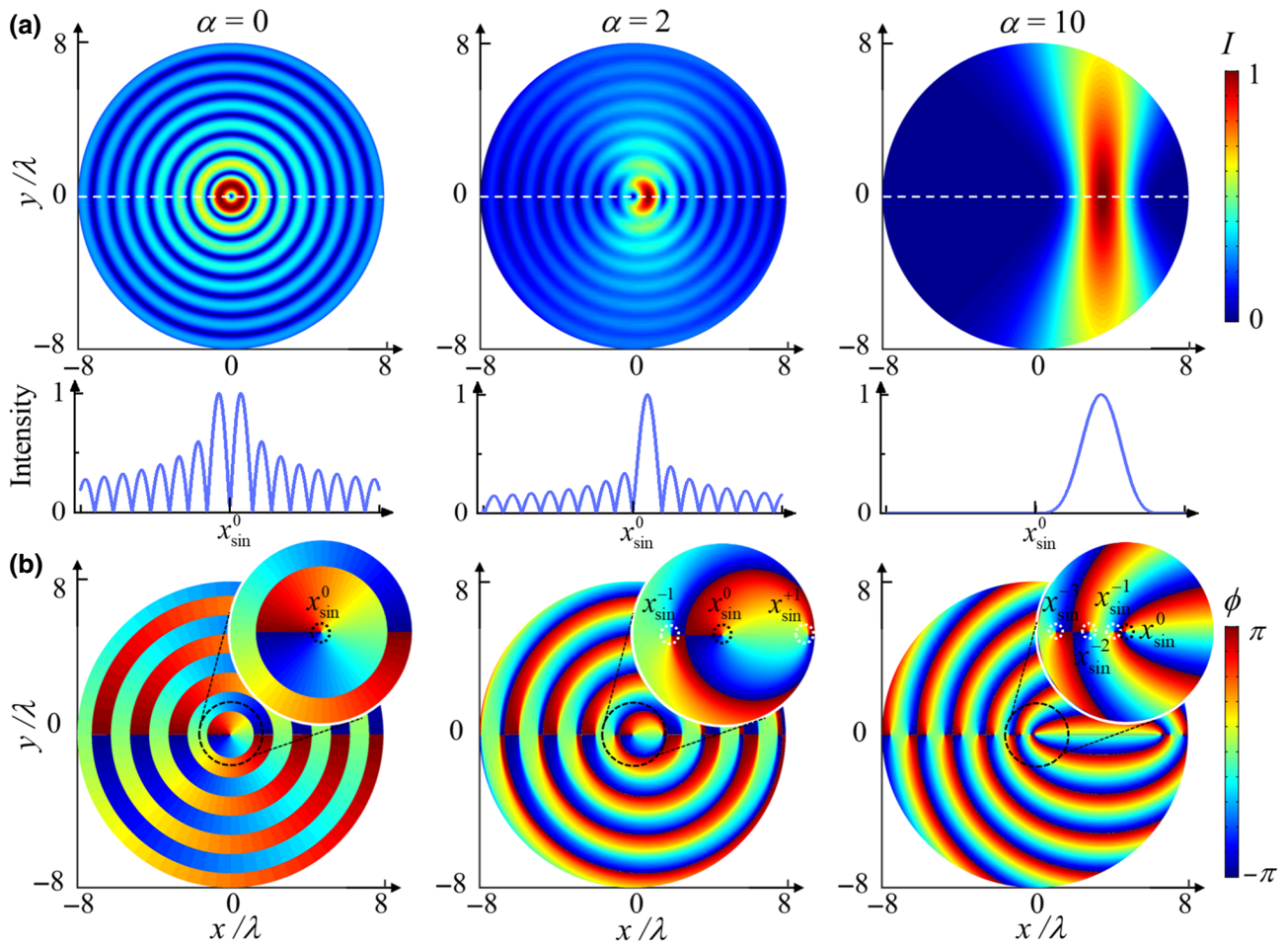


FIG. 1. (a) Normalized intensity and (b) phase distributions of the asymmetric acoustic vortices with the same topological charge  $l = 1$  but different asymmetry parameter ( $\alpha = 0, 2, 10$ ). The intensity distributions of the asymmetric vortices are featured with the crescent shape, and the asymmetry is increased with the parameter  $\alpha$ . Intensity profiles along the horizontal lines are plotted in the bottom of (a). Besides the ordinary singularity at the origin, the asymmetric vortex acquires several pairs of extra singularities on the  $x$  axis, with the opposite chirality on different sides of the origin. The insets in (b) are the enlarged views of the phase patterns with labeled singularities.

The positions of the extra singularities are calculated to be

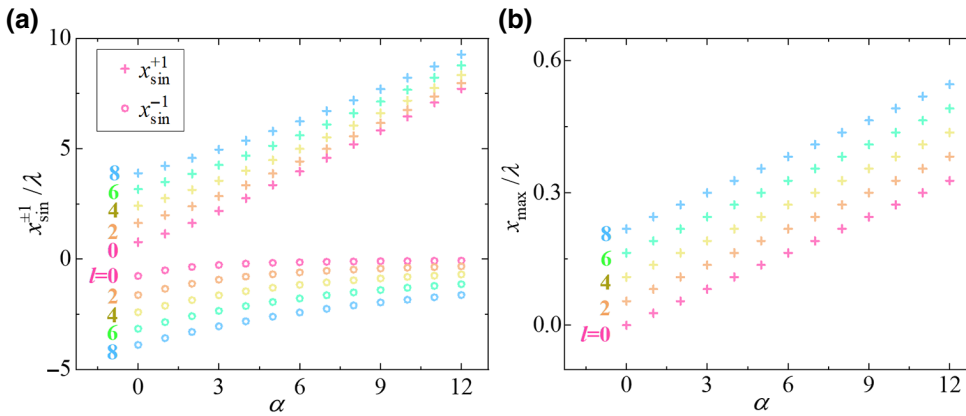
$$\begin{aligned} x_{\sin}^{+p} &= \frac{\alpha + \sqrt{\alpha^2 + \gamma_l^{p^2}}}{\mu} \quad (\varphi = 2p\pi), \\ x_{\sin}^{-p} &= \frac{\alpha - \sqrt{\alpha^2 + \gamma_l^{p^2}}}{\mu} \quad [\varphi = (2p + 1)\pi]. \end{aligned} \quad (6)$$

Significantly, for  $\alpha \neq 0$ , all the extra singularities give rise to acoustic vortices with unit topological charge and opposite signs on different sides of the origin [31]. When  $\alpha = 0$ , there are no isolated intensity nulls except for the one at the origin with topological charge  $l$ . Instead, the zero intensity is distributed along the concentric circumferences. Locations of the first pair of extra singularities  $x_{\sin}^{\pm 1}$  are illustrated in Fig. 2(a) as functions of  $l$  and  $\alpha$ . In addition, from Eq. (6), the singularities are asymmetrically distributed on the  $x$  axis since  $|x_{\sin}^+| > |x_{\sin}^-|$ . The asymmetry is growing with  $\alpha$ , agreeing with the results

in Fig. 1(a). The asymmetry can also be characterized by the shift of intensity peak. According to Eq. (4), the position of the intensity peak is approximated to be  $x_{\max} \approx (l + \alpha)/\mu$ , as illustrated in Fig. 2(b), which verifies the positive correlation between the asymmetry degree and the parameter  $\alpha$ .

#### IV. IMPLEMENTATION WITH ACOUSTIC METASURFACE

We design acoustic metasurface for practical implementation of the asymmetric vortex beam. Acoustic metasurface has been extensively studied in the generation of conventional symmetric vortex based on the physically spiral structures [6, 26, 27, 32–36]. In principle, the expression in Eq. (5) should be satisfied both in aspects of amplitude and phase for the perfect generation. However, the simultaneous manipulation of amplitude and phase is challenging



[37]. Research on acoustic conventional symmetric vortex show that the phase modulation plays a more important role than amplitude in the generation [3,6]. Therefore, we employ a feasible strategy for the implementation with the phase-only modulation metasurface [38–42], which has been proven to have good performances in many cases [43–45]. The metasurface is made of grooves with different depths to provide the phase delay in the reflected wave to satisfy the phase requirement in Eq. (5). Figure 3(d) shows the photograph of the metasurface sample fabricated by three-dimensional (3D) printing technology, and the schematic of the implementation is illustrated in Fig. 3(e).

Throughout this paper, we carry out the numerical simulations based on COMSOL Multiphysics software. Without losing generality, we consider the airborne sound of frequency 4000 Hz ( $\lambda = 8.6$  cm) propagating in air. Acoustic intensity patterns on the transverse plane ( $x$ - $y$  plane) of the asymmetric vortex beams ( $l = 1, \alpha = 2$ ) generated by the metasurface are demonstrated in Fig. 3(c), compared with the results for the ideal source and the phase-only source [Fig. 3(a) and 3(b)]. It is readily observed that the intensity preserves the crescent shape from near field ( $z = 0.1\lambda$ ) to far field ( $z = 7\lambda$ ) in Figs. 3(a) and 3(b), and the profiles along the  $x$  axis [Fig. 3(f)] agree well with the theory. In the generation with metasurface, the intensity evolves from the ambiguous distribution in the near field ( $z = 0.1\lambda$ ) into the clear crescent shape when  $z \geq 2\lambda$  [Fig. 3(c)].

We then discuss the nondiffractive nature of the asymmetric vortex. Theoretically, a single Bessel beam with the infinite energy is nondiffractive in free space [46]. Therefore, the proposed asymmetric vortex described by the Bessel function with the complex argument [Eq. (5)] should possess the same nondiffractive feature. Figure 3 shows that the intensity preserves the crescent shape from the very near field ( $z = 0.1\lambda$ ) to far field ( $z = 8\lambda$ ), which unambiguously proves the nondiffractive nature of the asymmetric vortex. Moreover, the intensity peaks shift by identical offsets in different propagating distances, consistent with the theoretical predictions. The discrepancy between the theory and simulation results may result from

FIG. 2. (a) Positions of the first pair of the extra singularities  $x_{\sin}^{\pm 1}$  in the asymmetric vortex beam as functions of topological charge  $l$  and asymmetry parameter  $\alpha$ .  $x_{\sin}^{+1}$  ( $x_{\sin}^{-1}$ ) indicates the extra singularities on right (left) of the origin with opposite chirality. (b) Maximum intensity position of the asymmetric vortex as functions of  $l$  and  $\alpha$ .

the phase-only control of the metasurface. The progress on acoustic metasurface with the effective manipulations of both phase and amplitude contributes to the generation of perfect asymmetry vortex beam.

## V. MODULATION OF OAM WITH ASYMMETRY

We further investigate the acoustic OAM carried in the asymmetric vortex beam. The OAM density per unit power projected onto the beam axis is given by [4,47,48]  $j_z = \omega \epsilon \text{Im}[\Psi(\partial\Psi^*/\partial\varphi)]$ , and the sound-energy density is  $\varsigma = \omega^2 \epsilon \Psi \Psi^*$ , where  $\epsilon = \rho_0/c_0^2$ . The total OAM and sound energy of the asymmetric vortex beam on the transverse planes are calculated to be

$$M_z = \text{Im} \left( \int_0^\infty \int_0^{2\pi} \omega \epsilon \psi \frac{\partial \psi^*}{\partial \varphi} r dr d\varphi \right), \quad (7)$$

$$E = \int_0^\infty \int_0^{2\pi} \omega^2 \epsilon \Psi \Psi^* r dr d\varphi. \quad (8)$$

The total OAM  $M_z$  and sound energy  $E$  are conservative during propagation, therefore, we can calculate the values in the initial plane. Substituting Eq. (2) into Eqs. (7) and (8), one obtains

$$M_z = 2\pi \omega \epsilon \sum_{m=0}^{\infty} \frac{\alpha^{2m} (l+m)}{(m!)^2} \int_0^\infty J_{l+m}^2(\mu r) r dr, \quad (9)$$

$$E = 2\pi \omega^2 \epsilon \sum_{m=0}^{\infty} \frac{\alpha^{2m}}{(m!)^2} \int_0^\infty J_{l+m}^2(\mu r) r dr. \quad (10)$$

Employing the reference integrals [49]

$$\int J_p^2(\mu r) r dr = \frac{r^2}{2} [J_p^2(\mu r) - J_{p-1}^2(\mu r) J_{p+1}^2(\mu r)], \quad (11)$$

and the asymptotic forms of the Bessel function at large argument, we deduce the ratio between the total OAM and

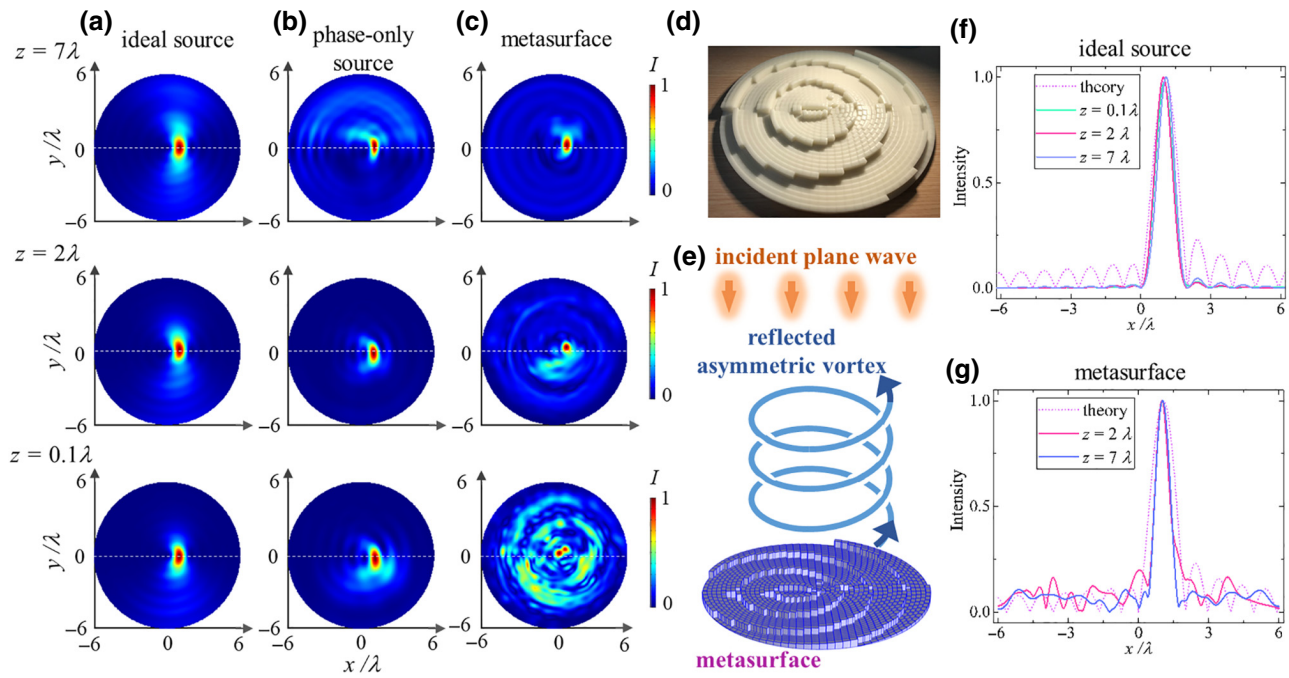


FIG. 3. Intensity distributions of the asymmetric acoustic vortex beams generated by (a) ideal source (b) phase-only source (c) metasurface on  $x$ - $y$  planes in different distances  $z = 0.1\lambda$ ,  $z = 2\lambda$ , and  $z = 7\lambda$ , with  $l = 1$ ,  $\alpha = 2$ . (d) Photograph of the metasurface sample. (e) Schematic of acoustic reflection metasurface. (f)–(g) Intensity profiles along the  $x$  axis for ideal source and metasurface.

sound energy on the transverse cross section into

$$\frac{\omega M_z}{E} = l + \sum_{m=0}^{\infty} \frac{\alpha^{2m} m}{(m!)^2} \left( \sum_{m=0}^{\infty} \frac{\alpha^{2m}}{(m!)^2} \right)^{-1} = l + \alpha \frac{I_1(2\alpha)}{I_0(2\alpha)}, \quad (12)$$

where  $I_n(x)$  is the modified Bessel function.

Equation (12) gives alternative insights of the OAM-to-energy ratio in the asymmetric acoustic vortex, which reveals the following features: (i) The OAM-to-energy ratio of the asymmetric vortex is *not* described by the ratio  $l/\omega$  as for the conventional symmetric vortex; (ii) The OAM is linearly increased with topological charge  $l$ , following the same behavior as the symmetric vortex; (iii) The asymmetry parameter  $\alpha$  contributes to the OAM as well. The larger asymmetry leads to the larger OAM; (iv) Counterintuitively, the asymmetric beam with topological charge  $l = 0$  can be endowed with finite OAM; (v) The effective topological charge of the asymmetric vortex, defined as  $\tilde{l} = l + \alpha I_1(2\alpha)/I_0(2\alpha)$ , can take both the integer or fractional values [26,27].

These features are demonstrated in Fig. 4, showing the value of  $\omega M_z/E$  as a function of asymmetry parameter  $\alpha$ . As predicted, the total axial OAM on the transverse plane of the beam is linearly proportional to  $l$ , and can be well controlled by  $\alpha$ , which provides an additional degree of freedom for acoustic OAM modulation.

## VI. SUMMARY

We report the theoretical proposal and numerical investigation of the asymmetric acoustic vortex beam based on the superposition of Bessel modes. We design the phase-only acoustic metasurface with satisfying performance for

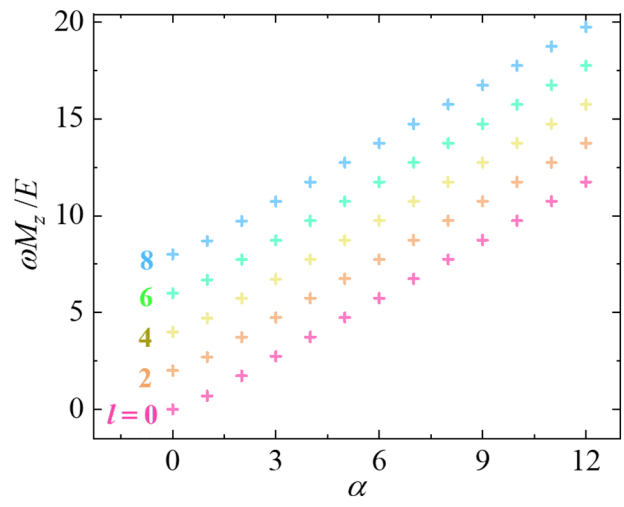


FIG. 4. Ratio between the total axial OAM  $M_z$  and sound energy  $E$  on the transverse plane, as functions of topological charge  $l$  and asymmetry parameter  $\alpha$ . The ratio is linearly dependent on  $l$ , in accordance with the conventional symmetric vortex. For a given  $l$ , the axial OAM  $M_z$  grows with  $\alpha$  as well, demonstrating an alternative factor for modulating the OAM.

the beam generation, which provides an effective prototype for the implementation in practical applications. We further find the anomalous singularity behavior of the asymmetric vortex with additional pairs of intensity nulls. Significantly, we reveal that the OAM of the asymmetric vortex is linearly proportional to topological charge  $l$  as the conventional vortex, but also depends on the beam asymmetry. Our work introduces the symmetry as an alternative factor for the acoustic OAM modulation beyond the topological charge  $l$ , which will be useful for applications of acoustic vortex in communications and particle manipulations.

## ACKNOWLEDGMENTS

The authors are grateful for helpful discussions with Dr. Likun Zhang at the University of Mississippi. This work is supported by National Natural Science Foundation of China (Grant No. 11904055, 11525416 and 11827808), Shanghai Committee of Science and Technology (Grant No. 20ZR1404200), Program of Shanghai Academic Research Leader (Grant No.19XD1400500), and the China Association for Science and technology (CAST).

- [1] J. F. Nye, M. V. Berry, and F. C. Frank, Dislocations in wave trains, *Proc. R. Soc. Lond. A. Math. Phys. Sci.* **336**, 165 (1974).
- [2] M. Berry, Making waves in physics, *Nature* **403**, 21 (2000).
- [3] B. T. Hefner and P. L. Marston, An acoustical helicoidal wave transducer with applications for the alignment of ultrasonic and underwater systems, *J. Acoust. Soc. Am.* **106**, 3313 (1999).
- [4] L. Zhang and P. L. Marston, Angular momentum flux of nonparaxial acoustic vortex beams and torques on axisymmetric objects, *Phys. Rev. E* **84**, 065601 (2011).
- [5] C. E. M. Demore, Z. Yang, A. Volovick, S. Cochran, M. P. MacDonald, and G. C. Spalding, Mechanical Evidence of the Orbital Angular Momentum to Energy Ratio of Vortex Beams, *Phys. Rev. Lett.* **108**, 194301 (2012).
- [6] X. Jiang, Y. Li, B. Liang, J. Cheng, and L. Zhang, Convert Acoustic Resonances to Orbital Angular Momentum, *Phys. Rev. Lett.* **117**, 034301 (2016).
- [7] M. Baudoin, J.-C. Gerbedoen, A. Riaud, O. B. Matar, N. Smagin, and J.-L. Thomas, Folding a focalized acoustical vortex on a flat holographic transducer: Miniaturized selective acoustical tweezers, *Sci. Adv.* **5**, eaav1967 (2019).
- [8] A. Marzo and B. W. Drinkwater, Holographic acoustic tweezers, *Proc. Natl. Acad. Sci. U. S. A.* **116**, 84 (2019).
- [9] L. Allen, M. W. Beijersbergen, R. J. C. Spreeuw, and J. P. Woerdman, Orbital angular momentum of light and the transformation of laguerre-Gaussian laser modes, *Phys. Rev. A* **45**, 8185 (1992).
- [10] M. R. Dennis, K. O'Holleran, and M. J. Padgett, in *Progress in Optics*, edited by E. Wolf (Elsevier, Amsterdam, 2009), pp. 293–363.

- [11] M. Uchida and A. Tonomura, Generation of electron beams carrying orbital angular momentum, *Nature* **464**, 737 (2010).
- [12] J. Verbeeck, H. Tian, and P. Schattschneider, Production and application of electron vortex beams, *Nature* **467**, 301 (2010).
- [13] B. J. McMorran, A. Agrawal, I. M. Anderson, A. A. Herzing, H. J. Lezec, J. J. McClelland, and J. Unguris, Electron vortex beams with high quanta of orbital angular momentum, *Science* **331**, 192 (2011).
- [14] A. Anhäuser, R. Wunenburger, and E. Brasselet, Acoustic Rotational Manipulation Using Orbital Angular Momentum Transfer, *Phys. Rev. Lett.* **109**, 034301 (2012).
- [15] A. Marzo, M. Caleap, and B. W. Drinkwater, Acoustic Virtual Vortices with Tunable Orbital Angular Momentum for Trapping of Mie Particles, *Phys. Rev. Lett.* **120**, 044301 (2018).
- [16] D. Baresch, J.-L. Thomas, and R. Marchiano, Orbital Angular Momentum Transfer to Stably Trapped Elastic Particles in Acoustical Vortex Beams, *Phys. Rev. Lett.* **121**, 074301 (2018).
- [17] A. Ozcelik, J. Rufo, F. Guo, Y. Gu, P. Li, J. Lata, and T. J. Huang, Acoustic tweezers for the life sciences, *Nat. Methods* **15**, 1021 (2018).
- [18] Z. Gong and M. Baudoin, Particle Assembly with Synchronized Acoustic Tweezers, *Phys. Rev. Appl.* **12**, 024045 (2019).
- [19] X. Jiang, B. Liang, J.-C. Cheng, and C.-W. Qiu, Twisted acoustics: Metasurface-enabled multiplexing and demultiplexing, *Adv. Mater.* **30**, 1800257 (2018).
- [20] C. Shi, M. Dubois, Y. Wang, and X. Zhang, High-speed acoustic communication by multiplexing orbital angular momentum, *Proc. Natl. Acad. Sci. U. S. A.* **114**, 7250 (2017).
- [21] X. Jiang, C. Shi, Y. Wang, J. Smalley, J. Cheng, and X. Zhang, Nonresonant Metasurface for Fast Decoding in Acoustic Communications, *Phys. Rev. Appl.* **13**, 014014 (2020).
- [22] L. Zhang, A general theory of arbitrary bessel beam scattering and interactions with a sphere, *J. Acoust. Soc. Am.* **143**, 2796 (2018).
- [23] A. T. O'Neil, I. MacVicar, L. Allen, and M. J. Padgett, Intrinsic and Extrinsic Nature of the Orbital Angular Momentum of a Light Beam, *Phys. Rev. Lett.* **88**, 053601 (2002).
- [24] X.-D. Fan, Z. Zou, and L. Zhang, Acoustic vortices in inhomogeneous media, *Phys. Rev. Res.* **1**, 032014 (2019).
- [25] S. Guo, X. Guo, X. Wang, X. Du, P. Wu, A. Bouakaz, and M. Wan, Manipulation of Nanodroplets via a Nonuniform Focused Acoustic Vortex, *Phys. Rev. Appl.* **13**, 034009 (2020).
- [26] Y.-R. Jia, Q. Wei, D.-J. Wu, Z. Xu, and X.-J. Liu, Generation of fractional acoustic vortex with a discrete archimedean spiral structure plate, *Appl. Phys. Lett.* **112**, 173501 (2018).
- [27] Y.-R. Jia, W.-Q. Ji, D.-J. Wu, and X.-J. Liu, Metasurface-enabled airborne fractional acoustic vortex emitter, *Appl. Phys. Lett.* **113**, 173502 (2018).
- [28] P. L. Marston, Axial radiation force of a bessel beam on a sphere and direction reversal of the force, *J. Acoust. Soc. Am.* **120**, 3518 (2006).

- [29] I. S. Gradshteyn, I. M. Ryzhik, Table of integrals, series, and products, *Table of Integrals, Series, and Products* (Academic Press, 2014).
- [30] V. V. Kotlyar, A. A. Kovalev, and V. A. Soifer, Asymmetric bessel modes, *Opt. Lett.* **39**, 2395 (2014).
- [31] V. V. Kotlyar, A. A. Kovalev, R. V. Skidanov, and V. A. Soifer, Asymmetric bessel-gauss beams, *JOSA A* **31**, 1977 (2014).
- [32] X. Jiang, J. Zhao, S. Liu, B. Liang, X. Zou, J. Yang, C.-W. Qiu, and J. Cheng, Broadband and stable acoustic vortex emitter with multi-arm coiling slits, *Appl. Phys. Lett.* **108**, 203501 (2016).
- [33] L. Ye, C. Qiu, J. Lu, K. Tang, H. Jia, M. Ke, S. Peng, and Z. Liu, Making sound vortices by metasurfaces, *AIP Adv.* **6**, 085007 (2016).
- [34] N. Jiménez, V. Romero-García, L. M. García-Raffi, F. Camarena, and K. Staliunas, Sharp acoustic vortex focusing by fresnel-spiral zone plates, *Appl. Phys. Lett.* **112**, 204101 (2018).
- [35] J. Li, A. Díaz-Rubio, C. Shen, Z. Jia, S. Tretyakov, and S. Cummer, Highly Efficient Generation of Angular Momentum with Cylindrical Biaxialotropic Metasurfaces, *Phys. Rev. Appl.* **11**, 024016 (2019).
- [36] Y. Jin, R. Kumar, O. Poncelet, O. Mondain-Monval, and T. Brunet, Flat acoustics with soft gradient-index metasurfaces, *Nat. Commun.* **10**, 1 (2019).
- [37] Y. Zhu, J. Hu, X. Fan, J. Yang, B. Liang, X. Zhu, and J. Cheng, Fine manipulation of sound via lossy metamaterials with independent and arbitrary reflection amplitude and phase, *Nat. Commun.* **9**, 1 (2018).
- [38] G. Ma, M. Yang, S. Xiao, Z. Yang, and P. Sheng, Acoustic metasurface with hybrid resonances, *Nat. Mater.* **13**, 873 (2014).
- [39] Y. Xie, W. Wang, H. Chen, A. Konneker, B.-I. Popa, and S. A. Cummer, Wavefront modulation and subwavelength diffractive acoustics with an acoustic metasurface, *Nat. Commun.* **5**, 5553 (2014).
- [40] Y. Li, X. Jiang, R. Li, B. Liang, X. Zou, L. Yin, and J. Cheng, Experimental Realization of Full Control of Reflected Waves with Subwavelength Acoustic Metasurfaces, *Phys. Rev. Appl.* **2**, 064002 (2014).
- [41] Y.-F. Zhu, X.-Y. Zou, R.-Q. Li, X. Jiang, J. Tu, B. Liang, and J.-C. Cheng, Dispersionless manipulation of reflected acoustic wavefront by subwavelength corrugated surface, *Sci. Rep.* **5**, 1 (2015).
- [42] Y. Li, X. Jiang, B. Liang, J. Cheng, and L. Zhang, Metascreen-Based Acoustic Passive Phased Array, *Phys. Rev. Appl.* **4**, 024003 (2015).
- [43] P. Zhang, T. Li, J. Zhu, X. Zhu, S. Yang, Y. Wang, X. Yin, and X. Zhang, Generation of acoustic self-bending and bottle beams by phase engineering, *Nat. Commun.* **5**, 4316 (2014).
- [44] K. Melde, A. G. Mark, T. Qiu, and P. Fischer, Holograms for acoustics, *Nature* **537**, 518 (2016).
- [45] H. Gao, Z. Gu, B. Liang, X. Zou, J. Yang, J. Yang, and J. Cheng, Acoustic focusing by symmetrical self-bending beams with phase modulations, *Appl. Phys. Lett.* **108**, 073501 (2016).
- [46] Z. Bouchal and M. Olivík, Non-diffractive vector bessel beams, *J. Mod. Opt.* **42**, 1555 (1995).
- [47] J.-L. Thomas, T. Brunet, and F. Coulouvrat, Generalization of helicoidal beams for short pulses, *Phys. Rev. E* **81**, 016601 (2010).
- [48] L. Zhang, Reversals of Orbital Angular Momentum Transfer and Radiation Torque, *Phys. Rev. Appl.* **10**, 034039 (2018).
- [49] M. Abramowitz, I. A. Stegun, Handbook of mathematical functions with formulas, graphs, and mathematical tables, *Handbook of Mathematical Functions with Formulas, Graphs, and Mathematical Tables* (U.S. Government Printing Office, Washington D. C., 1948).